www.MINEPORTAL.in

(All Mining Solutions)

- **ONLINE TEST SERIES FOR**
  - **DGMS COAL/METAL FIRST & SECOND CLASS**
  - **GATE MINING**
  - **COAL INDIA EXAMS**
  - **OTHER MINING EXAMS**
- **ONLINE ORDER MINING BOOKS AT GREAT DISCOUNT**
- **FREE STUDY MATERIAL**
- **WHATSAPP CHAT SUPPORT FOR MINING EXAMS & QUERY RELATED TO MINING**

VISITING SITE- www.MINEPORTAL.in

fb- www.fb.com/mineportal.in

CALL/WHATSAPP- 8804777500

EMAIL- INFO@MINEPORTAL.IN

ROCK DISCONTINUITIES

1. INTRODUCTION

1.1 Effect of Discontinuities on Rock Mass Properties

Rock masses are far from being continua and consist essentially of two constituents: intact rock and discontinuities (planes of weakness). The existence of one or several sets of discontinuities in a rock mass creates anisotropy in its response to loading and unloading. Also, compared to intact rock, jointed rock shows a higher permeability, reduced shear strength along the planes of discontinuity and increased deformability and negligible tensile strength in directions normal to those planes. Furthermore, discontinuities create scale effects. Finally, discontinuities form blocks by intersection that can result in stability problems during surface or underground excavations.

With few exceptions, it is incorrect to ignore the presence of discontinuities when modeling rock mass response to loading and unloading. Three approaches can be followed to account for the effect of discontinuities on rock mass strength and deformability.

The *first* approach consists of empirically reducing the deformability and strength properties of rock masses from those measured on intact rock samples in the laboratory. Rock mass modulus and strength can be estimated in different ways. For instance, Bieniawski and Orr (1976), Bieniawski (1978) and Serafim and Pereira (1983) proposed relationships between the modulus of deformation of rock masses and their *RMR* ratings using the geomechanics classification system (Bieniawski, 1974, 1993). Based on an extensive literature review, Heuze (1980) concluded that the modulus of deformation of rock masses ranges between 20 and 60 % of the modulus measured on intact rock specimens in the laboratory. Hoek and Brown (1980b) proposed an empirical failure criterion for rock masses containing two parameters m and s that are related to the degree of rock mass fracturing. Empirical expressions have also been proposed between those parameters and the Rock Quality Designation (*RQD*) and the *RMR* and *Q* ratings of Bieniawski (1974) and Barton et al. (1974). Although still the most reliable, the empirical approach lacks a mechanistic basis.

A *second* approach consists of treating joints as discrete features (Goodman et al., 1968; Heuze and Barbour, 1982). This is usually done in numerical methods such as the finite element, boundary element and discrete element methods in which the complex response of joints to normal and shear stresses can be introduced in an explicit manner. The main drawback of this approach is that only rock masses with a limited amount of joints can be analyzed due to computer limitations.

The *third* approach is to treat jointed rock as an equivalent anisotropic continuum with deformability and strength properties that are directional and also reflect the properties of intact rock and those of the joint sets, i.e. orientation, spacing and normal and shear stiffnesses. The discontinuities are characterized without reference to their specific locations. This approach was already discussed in Lecture Notes 5.

1.2 Classification of Discontinuities

Planes of weakness in rock are formed through failure in extension/tension, shear or in more complex failure modes that involve a combination of both. Failure surfaces formed in shear are usually smooth with some gouge material whereas failure surfaces formed in extension are rough and usually clean. Once formed, planes of weakness are more susceptible to weathering than the intact rock.

The properties of planes of weakness that affect the engineering behavior of rock structures include: (i) scale, frequency, continuity, density, spacing, (ii) roughness, type and degree of infilling, moisture conditions, hardness and degree of weathering, (iii) mechanical properties (shear strength and deformability) and hydraulic properties (permeability or conductivity) and, (iv) orientation.

Different terminologies are used by geologists, engineers and engineering geologists to describe the different types of planes of weakness in rocks. The term "discontinuities" is often used as a collective term for all structural breaks in geologic materials which usually have zero or low tensile strength. The term "joint" is also used as a generic term by rock engineers to include such structural breaks. The terminology and the descriptive criteria used here are those recommended by the U.S. Bureau of Reclamation for engineering works (see Table 1).

Discontinuities can be separated into five groups: fractures, shears, faults, shear/fault zones and shear/fault disturbed zones based on the mode of discontinuity movement and the scale of the discontinuities. The fractures are themselves divided into several groups based on rock core observation.

Note that joints often occur in sets. In each set, the joints have approximately the same orientation and usually the same character. Rock masses can contain several joint sets and some of them may be dominant. Several joint sets are frequent in igneous and metamorphic rock masses and can have special patterns such as columnar joints formed during the cooling of lava beds or sheet joints that are extension features resulting from the unloading near the free surfaces of massive rock masses.

1.3 Properties of Discontinuities

Fracture Frequency

Fracture frequency is defined as the number of natural fractures occurring within a base length or core run. The number of fractures is divided by the length and is reported as number of fractures per foot or fractures per meter. Fracture frequency is expressed as three fractures per meter or six fractures per foot. The fracture frequency has been related to the Rock Quality Designation Index (*RQD*) as follows (Priest and Hudson, 1976)

$$RQD = 100e^{-0.1\lambda}(0.1\lambda+1) \quad (1)$$

where 8 is defined as the number of fractures per meter determined on scanline surveys.

Fracture Density

A total of 10 descriptors are used to describe fracture density (see Table 1). The descriptors are obtained by examining the core recovery lengths in boreholes.

Fracture Spacing

Fracture spacing corresponds to the shortest distance between two consecutive fractures. Care should be taken to measure the true spacing instead of the apparent spacing. The difference is illustrated in Figures 1a and 1b for a rock mass intersected by a single joint set. If the orientation of the joints is known, true and apparent spacings are related.

For the geometry of Figure 1b, the *apparent fracture frequency*, $F = 1/S_a$, along the borehole, is related to the joint set dip angle, ", and the joint set spacing, *S*, as follows

$$F = \frac{1}{S_a} = \frac{\cos\alpha}{S} = f.\cos\alpha \qquad (2)$$

where $f = 1/S$ is the *true fracture frequency* measured in a direction perpendicular to the joint set. This equation can be generalized to the case of a borehole oriented at any angle with respect to a joint set of spacing *S* and of given orientation. Let n_1, n_2, n_3 be the direction cosines of the normal to a joint set and l_h, m_h, n_h be the direction cosines of a unit vector parallel to the borehole axis. The fracture frequency in the borehole direction is given by

$$F = \frac{l_h n_1 + m_h n_2 + n_h n_3}{S} \qquad (3)$$

Fracture Continuity

Discontinuities rarely cross entire rock masses and often terminates or branch and form bridges of intact rock.

Fracture Openness, Infilling and Healing

The openness of a fracture and the type and amount of infilling material have an effect on its hydraulic behavior and shear strength properties. Clean and tight fractures are usually less pervious and have higher shear strengths than open and filled discontinuities. It is also important to distinguish between the major types of fracture infilling. Brekke and Howard (1973) distinguished seven different types of filling material that can result in several engineering problems during underground excavation:

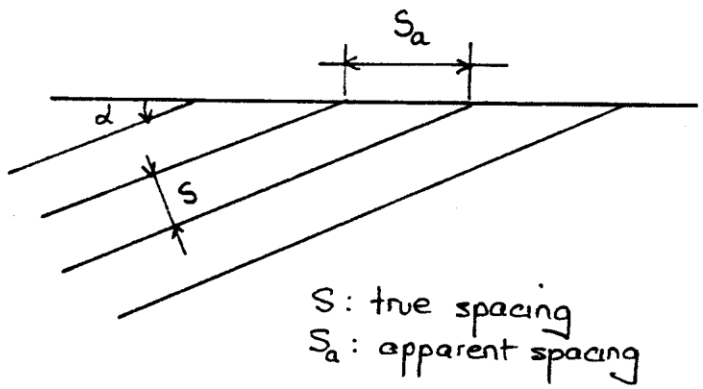

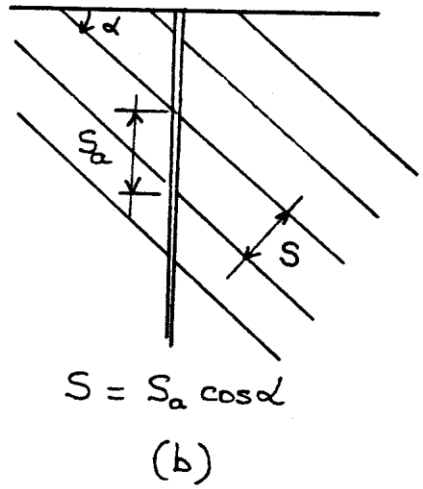

Figure 1. Difference between apparent and true fracture spacings for a rock mass cut by a single joint set (a) Apparent spacing measured from ground survey, (b) Apparent spacing measured in a borehole.

- Epidote, quartz, calcite which tend to "weld" the discontinuity walls together. These minerals can also be present without healing it;

- Clean discontinuities without filling or coatings;

- Calcite fillings may, especially when they are porous or flaky, dissolve during the lifetime of a project. Thus, their contribution to the shear strength may disappear with time. Gypsum fillings may behave the same way;

- Coatings or filings of chlorite, talc, graphite or serpentine make discontinuities very slippery (i.e. low strength) when wet;

- Inactive clay material in seams and faults naturally represents a very weak material that may squeeze or be washed out;

- Swelling clays may cause serious problems through free swell and consequent loss of strength, or through considerable swelling pressure when confined;

- Material that has been altered to a more cohesionless material (sand-like) may run or flow into the tunnel immediately following excavation.

Fracture Moisture Conditions

Flow in a rock mass is essentially along discontinuities. Different descriptors can be used to describe the amount of water along discontinuities varying from dry conditions to continuous flow (in which case the amount of water must be estimated).

Fracture Roughness

As for fracture openness and infilling, fracture roughness controls the shear strength of rock discontinuities. Rough discontinuities have higher shear strength than smooth ones. Fracture roughness can also be quantified using a *Joint Roughness Coefficient* Index (*JRC*) introduced by Barton and Choubey (1977). The latter varies between 0 and 20 and is obtained by comparing the discontinuity roughness profile to a series of reference profiles as shown in Figure 2.

Fracture Surface Hardness

Fracture surface hardness can be determined by conducting Schmidt Rebound Hammer Tests directly on the surface of rock discontinuities. Comparison between hardness measurements on different parts of a fracture surface can give an indication of the degree of surface weathering.

Shear and Fault Gauge Consistency

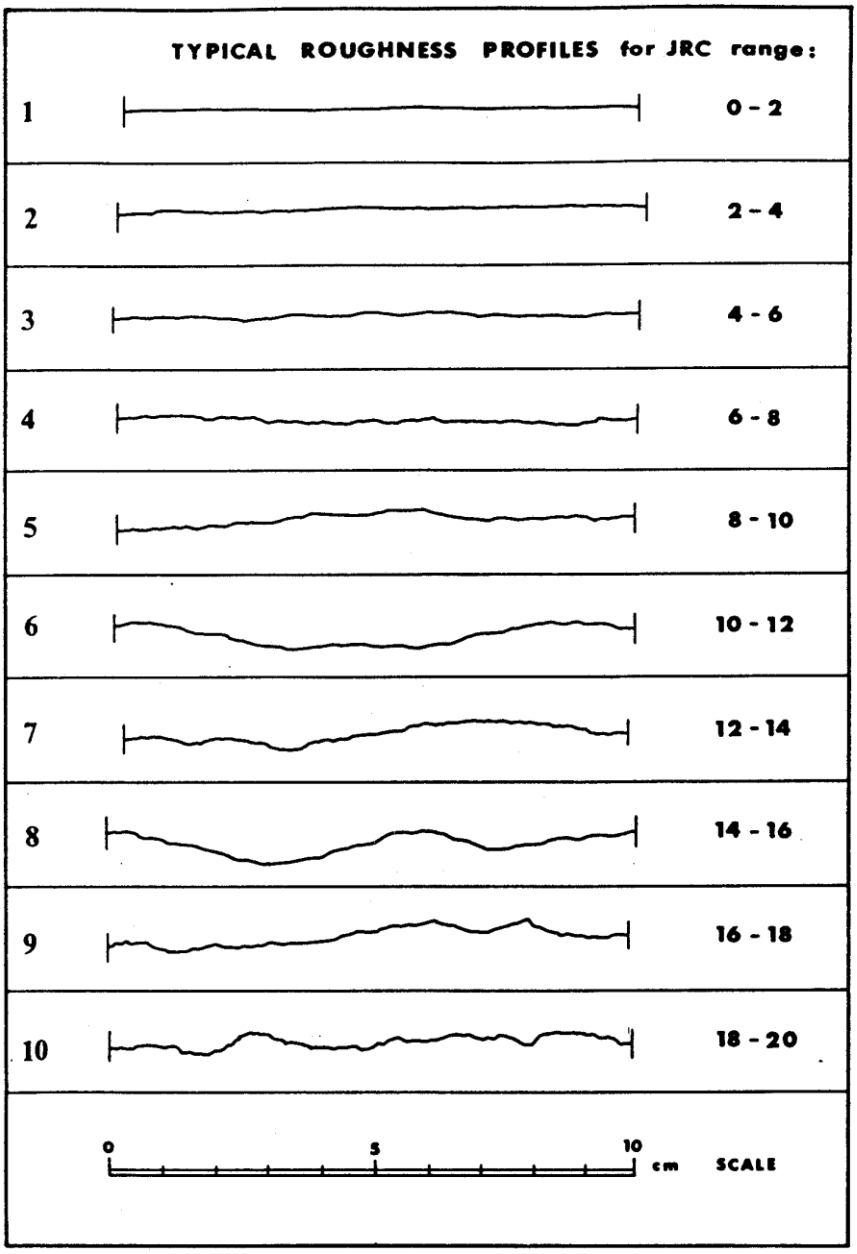

Figure 2. Roughness profiles and values of the *JRC* index as suggested by Barton and Choubey (1977).

Discontinuity Orientation

Discontinuities are usually planar and their orientation can be defined by two angles (i) strike and dip angles, or (ii) dip direction and dip angles. These angles are defined in Figure 3a.

- *Strike* - the compass direction of a line formed by the intersection of a horizontal plane and an inclined geologic plane such as a fault, fracture, joint, etc.. Because it is a compass direction, the strike is usually expressed relative to North or South. Hence, strike is expressed as "North (or South) so many degrees East" or "North (or South) so many degrees West"

- *Dip* - the angle between a horizontal plane and the plane of interest. As shown in Figure 3a, a thin stream of water poured on an inclined surface always runs down parallel to dip. The inclination of the water line down from the horizontal plane is called the (true) *dip angle*. The true dip angle is always measured perpendicular to the strike line.

- *Dip Direction* - The angle between North and the direction that the water runs down an inclined geologic plane. It is measured clockwise and varies between 0 and 360°.

- *Apparent Dip* - The inclination angle of a line on an inclined geologic plane measured in a direction oblique to the strike direction (Figure 3b). It varies between the true dip and 0°.

The orientation of a plane is shown on maps using a T-shaped symbol (Figure 3a); the long line of the symbol indicates the strike direction, and the short line shows the dip direction.

Strength and Deformability

Of particular interest when modeling the mechanical response of rock masses is the shear strength of rock discontinuities, and their deformability in the shear and normal directions (see Section 3).

2. SAMPLING AND TESTING OF ROCK DISCONTINUITIES

2.1 Sampling

The goal is to obtain samples of rock joints that are the least disturbed by the process of sampling. The different methods that can be used for sampling joints for laboratory testing are summarized in Figure 4 and consist of:

- oriented drilling of natural fractures (Figure 4a);
- integral sampling of natural fractures as proposed by Rocha and Franciss (1977) (Figure 4b);
- block cutting of natural fractures (Figure 4c);
- artificial joints produced by wire sawing or Brazilian splitting (Figure 4d);
- molding of fracture surface and replicas using plaster, sulfur or cement (Figure 4e).

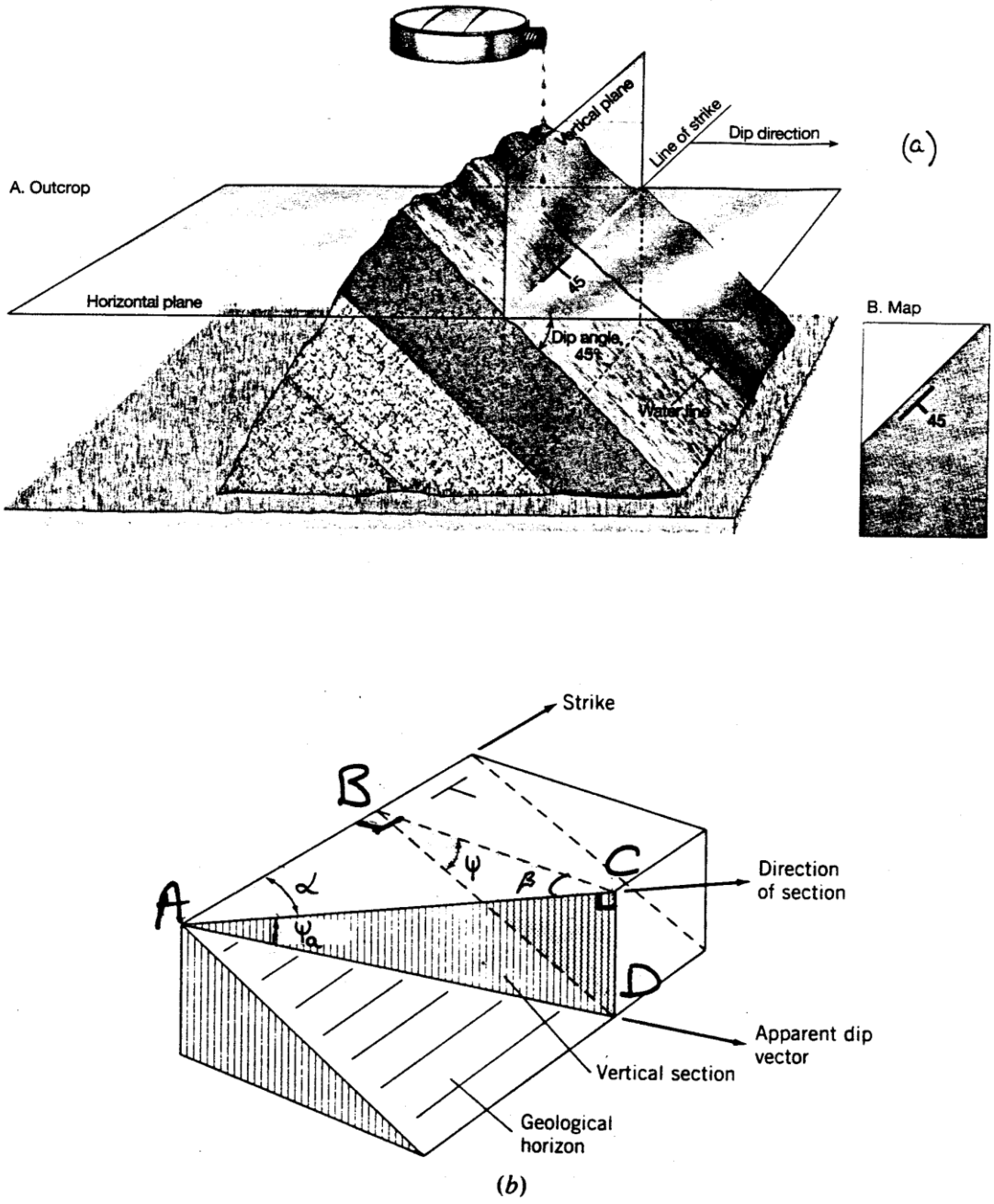

Figure 3. (a) Block diagram showing the strike, dip and dip direction angles of a geologic plane (after Hozik et al., 1996) (b) Definition of the apparent dip R_a in a direction " with respect to the strike line (after Goodman, 1993).

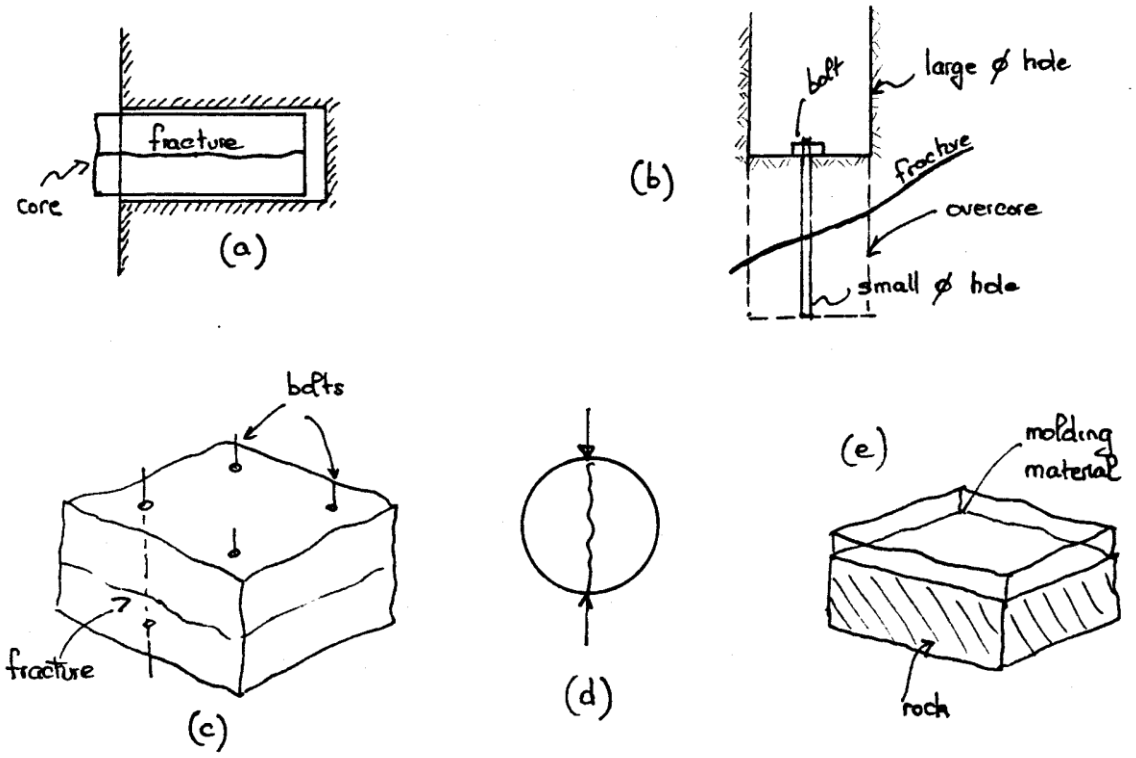

Figure 4. Methods used in the sampling of fractures.

2.2 Testing for Deformability and Strength

Normal Deformation of Rock Fractures

Rock fractures tend to close under compressive loading with a non-linear load displacement response curve. The amount of normal displacement is also controlled by the degree of fracture unmating or mismatching. In general, an unmated joint is more deformable than a mated one. The difference in normal behavior is illustrated in Figure 5 using experimental results adapted from Goodman (1976) where the normal stress normal displacement curves are shown for an intact rock specimen, a rock
specimen with a mated fracture and a mated specimen with an unmated fracture. The slope of the normal stress vs. displacement curve is called the normal stiffness. It is expressed in units of stress per length such as MPa/m or psi/in. Note that the normal stiffness of a fracture is not constant but increases with the normal stress level.

Joint Shear Deformation and Dilatancy

The shear response of rock fracture is usually obtained by using a *direct shear machine* or *shear box* such as that shown in Figure 6. The two halves of a fracture are cast in two platens using plaster, sulfur or other molding compounds. A normal load, *N*, is applied across the horizontal fracture. A shear load, *T*, is then applied and the fracture shear displacement and normal displacement are recorded. At the end of the shear test, a larger normal load is applied and the test is repeated.

The normal and shear load are usually expressed in terms of normal and shear stresses by dividing *N* and *T* by the total area of the joint (area of a mean plane passing through the hills and over the valleys of the fracture surface). The shear stress and normal displacement are usually plotted versus the horizontal shear displacement. Figure 7a shows the shear stress vs. displacement and normal displacement vs. shear displacement (dilation response) of a tension fracture(joint) tested by Barton (1976).

The shear stress vs. displacement curve in Figure 7a shows pre-peak, peak and post-peak regions. As shearing takes place, the fracture contracts first and dilates with a maximum rate of dilation at the peak shear strength. The actual response curves in Figure 7a have been idealized in Figure 7b. The slope of the pre-peak region is defined as the unit shear stiffness k_s and (J_p, u_p) and (J_r, u_r) are the shear stress and displacement components for the peak and residual conditions, respectively.

In general, the shear stiffness, the peak and residual shear strengths vary with the normal stress. Two models of variation of these quantities with the normal stress are shown in Figure 8a and 8b, respectively. In Figure 8a, the shear stiffness is constant whereas in Figure 8b, the shear stiffness increases with the normal stress. Criteria have been proposed to model the variation of the peak and residual shear strengths with the normal stress.

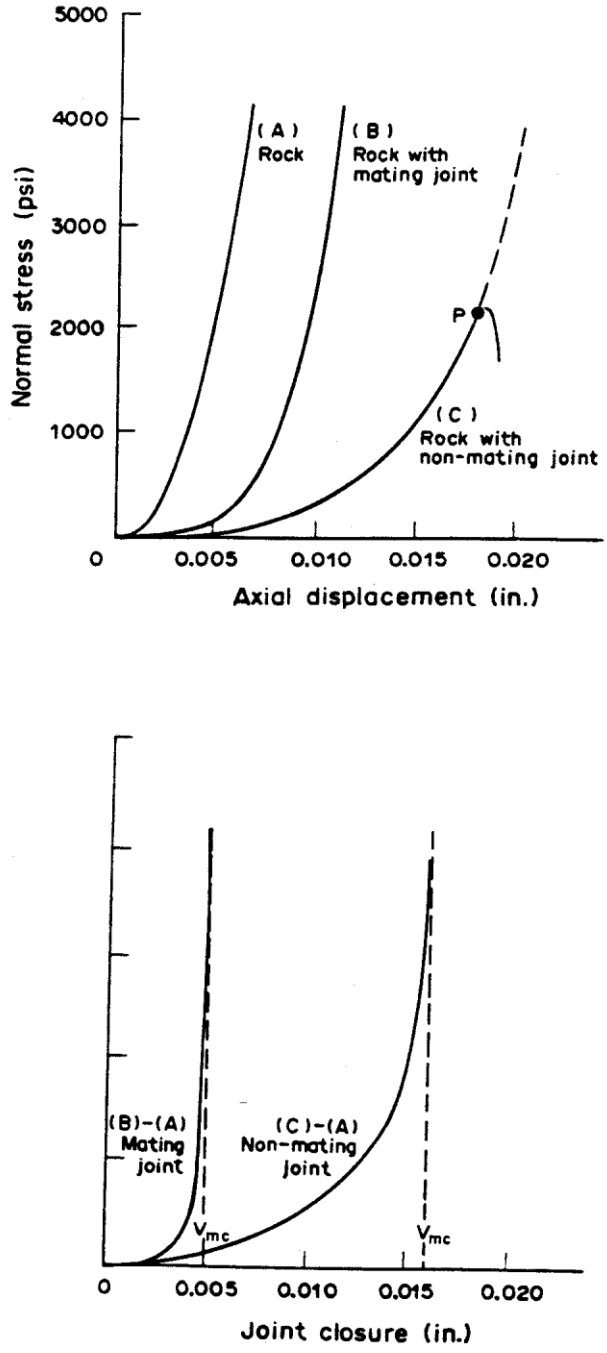

Figure 5. Normal stress normal displacement curves for an intact rock specimen, a rock specimen with a mated fracture and a rock specimen with an unmated fracture (after Goodman, 1976).

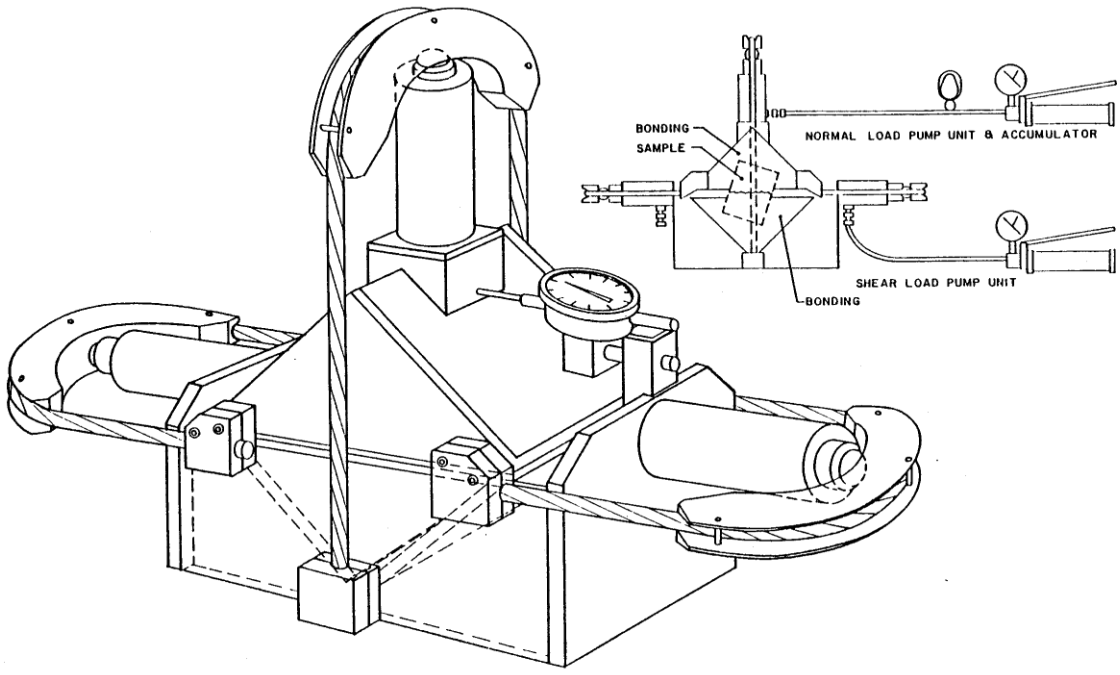

Figure 6. Direct shear box.

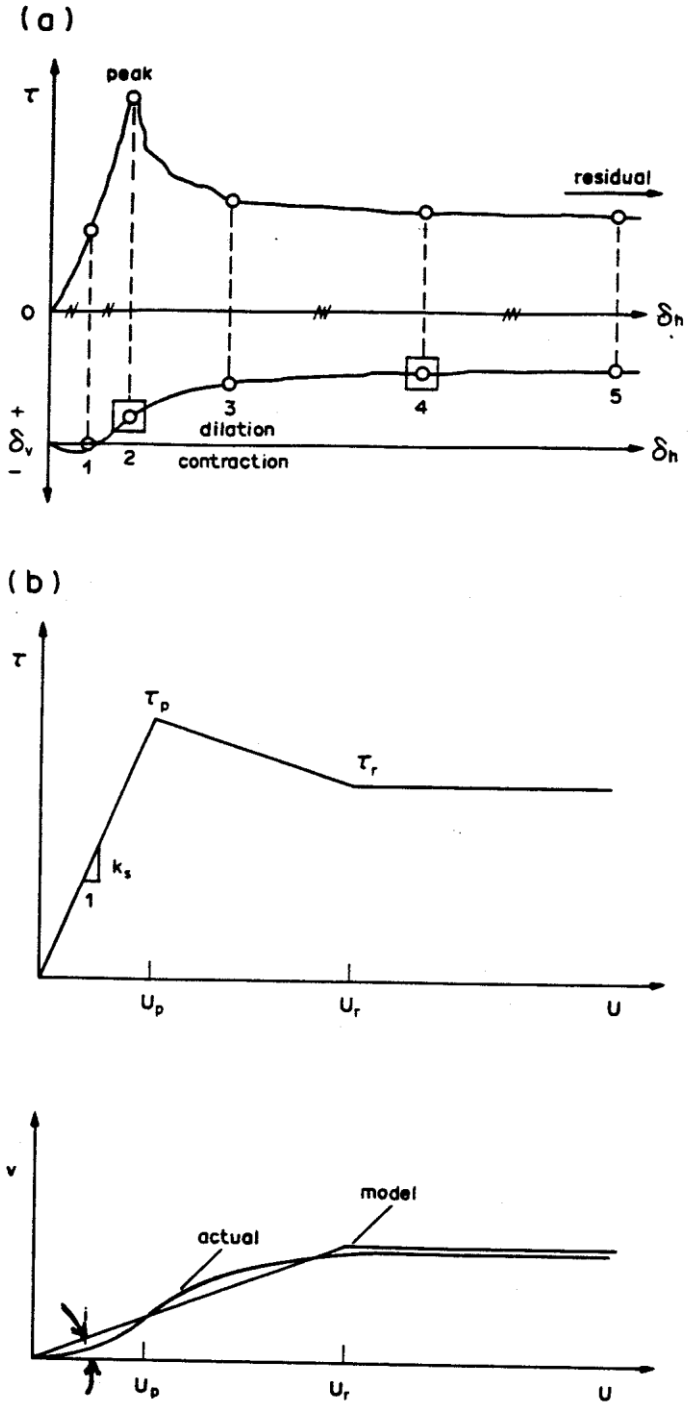

Figure 7. (a) Typical results of direct shear tests on a tension fracture (after Barton (1976)). (b) Idealized shear stress vs. shear displacement and dilatancy curves.

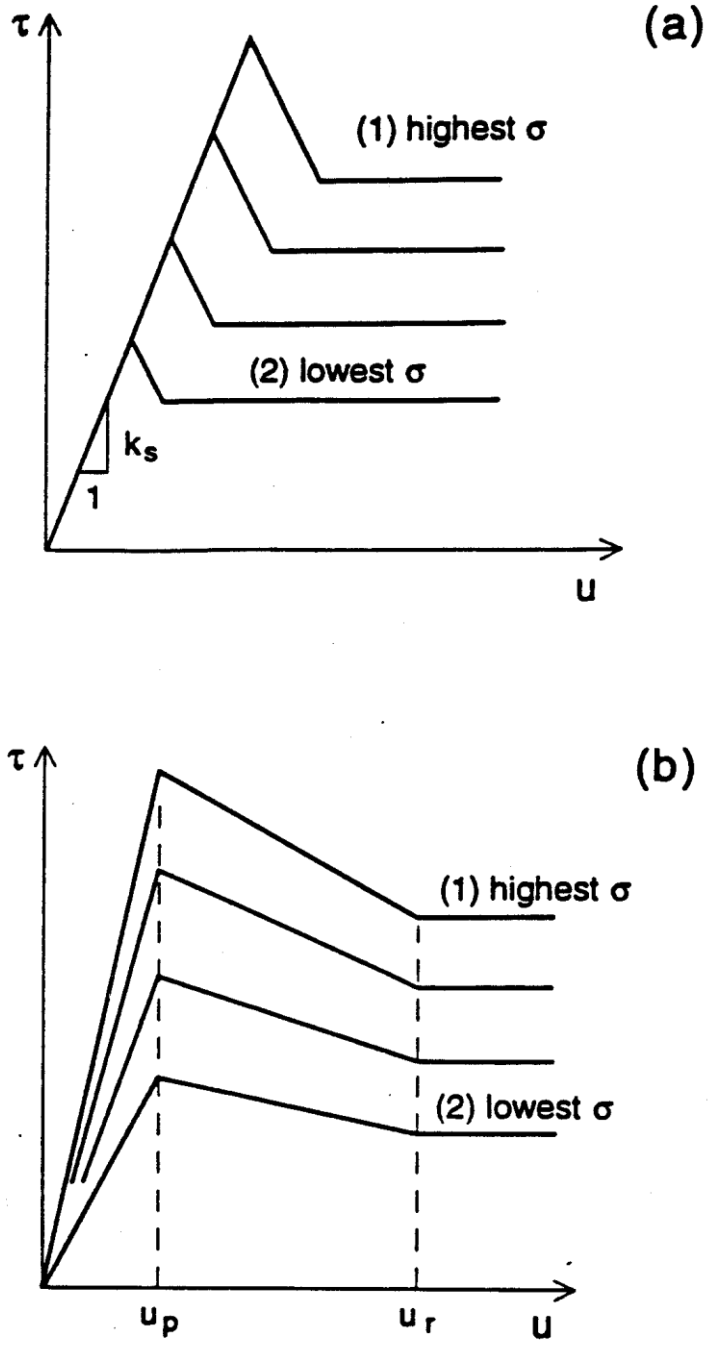

Figure 8. Shear stress vs. shear displacement models (a) Constant stiffness model, (b) Constant displacement model (after Goodman, 1976).

The shear response of rock fractures can also be determined by conducting triaxial tests on rock cores containing a joint inclined at an angle to the core axis (Figure 9a). Under an axisymmetric state of stress F_1 and $F_2 = F_3 = p$, the normal and shear stresses acting across a joint inclined at an angle * to F_1 are equal to

$$\sigma_n = \frac{(\sigma_1+\sigma_3)}{2} + \frac{(\sigma_3-\sigma_1)}{2}\cos 2\delta$$

$$\tau = \frac{(\sigma_1-\sigma_3)}{2}\sin 2\delta \qquad (4)$$

For a constant confining stress $F_3 = p$, an increase in F_1 results in an increase in both F_n and J. The corresponding stress path in the (F_n, J) space of Figure 9b is linear and extends until slip along the joint takes place. Experiments can be repeated for different values of the confining pressure *p*. This test is sometimes called a *multistage triaxial test.*

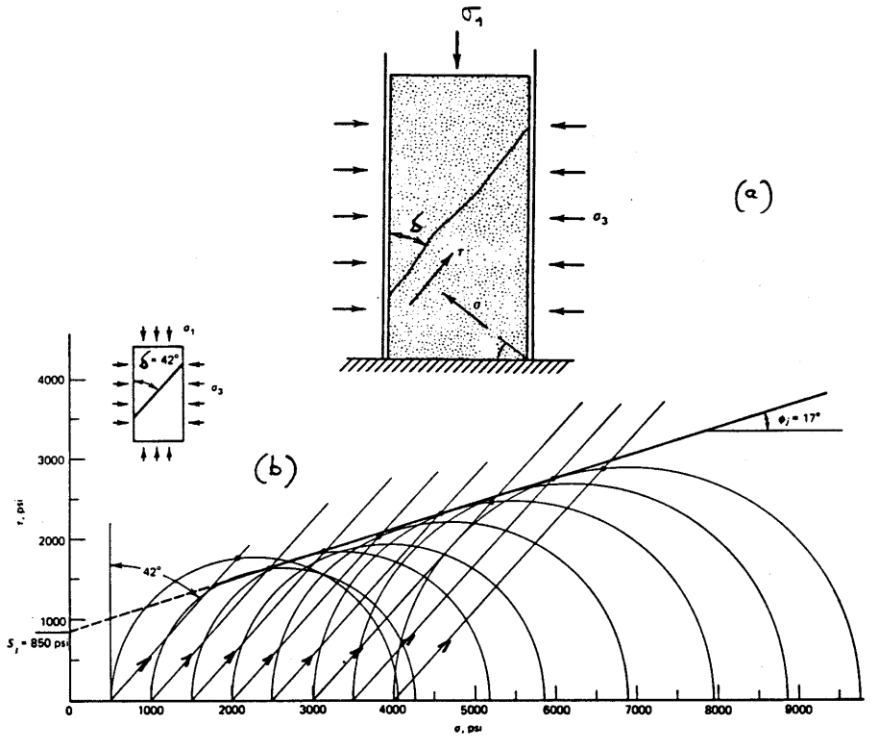

Figure 9. Multistage triaxial testing of a jointed rock specimen.

2.3 Effect of Boundary Conditions

Rock joints can be subject to different types of boundary conditions in the field ranging from constant normal stress to constant normal displacement (see Figure 10). Joint shear strength depends on the nature of those boundary conditions.

Methods to predict the shear behavior of rock joints under different conditions from the results of direct shear tests under constant normal stress can be found in Goodman (1989) and Saeb and Amadei (1992). In general, the shear strength of a joint under constant stiffness or displacement boundary conditions is higher than its shear strength under constant normal stress.

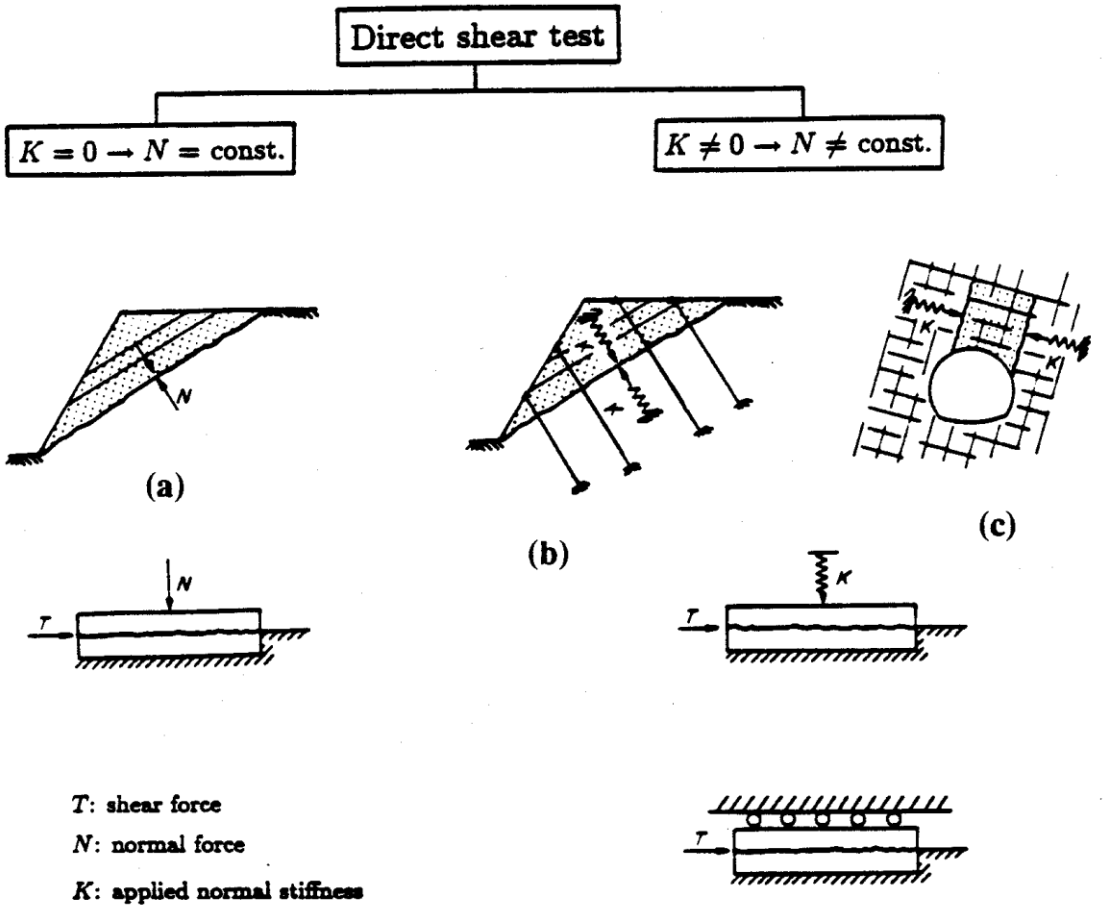

Figure 10. Range of boundary conditions across a joint surface.

3. SHEAR STRENGTH CRITERIA FOR ROCK DISCONTINUITIES

A number of criteria have been proposed to describe the variation of the peak shear strength with the applied normal stress. Similar criteria are also used for the residual shear strength.

3.1 Amonton's Law (1699)

For a surface, the frictional resistance is proportional to the applied normal load and independent on the apparent area of contact. In terms of stresses

$$\tau_p = \mu \ \sigma_n \tag{5}$$

where $\mu = \tan\phi_\mu$ is the coefficient of friction and ϕ_μ is the friction angle. A cohesion, c_j, can be added to the shear strength.

3.2 Newland and Alleyly (1957)

For rough surfaces, and assuming that the sliding surface consists of a series of sawtooth irregularities with an average angle i (see Figure 11), equation (5) is replaced by the following

$$\tau_p = \sigma_n \ \tan(\phi_\mu + i) \tag{6}$$

3.3. Patton (1966)

A bilinear model was proposed for rough surfaces that accounts for two phenomena that have been observed experimentally: (i) overriding of asperities at low normal stress levels and (ii) shearing through asperities at higher normal stress levels.

$$\begin{aligned} \tau_p &= \sigma_n \tan(\phi_\mu + i) \qquad when \quad \sigma_n < \sigma_t \\ \tau_p &= c_j + \sigma_n \tan\phi_r \qquad when \quad \sigma_n > \sigma_t \end{aligned} \tag{7}$$

where ϕ_r, ϕ_μ, c_j and i are defined in Figure 12. For most practical purposes, $\phi_r = \phi_\mu$.

3.4. Ladanyi and Archambault (1970)

$$\tau_p = \frac{\sigma_n(\bar{v} + \tan\phi_\mu)(1 - a_s) + a_s s_r}{1 - (1 - a_s)\bar{v} \ \tan\phi_\mu} \tag{8}$$

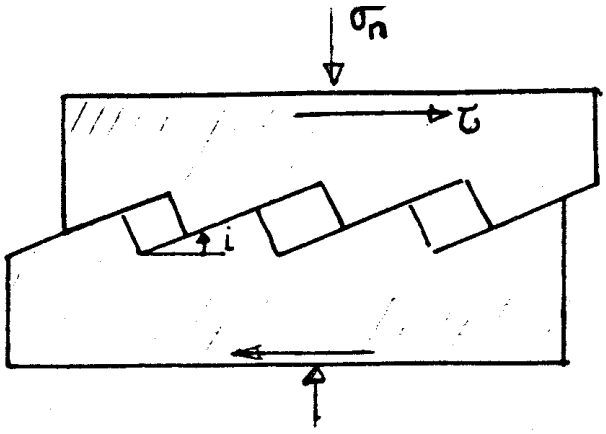

Figure 11. Shearing along a sawtooth surface.

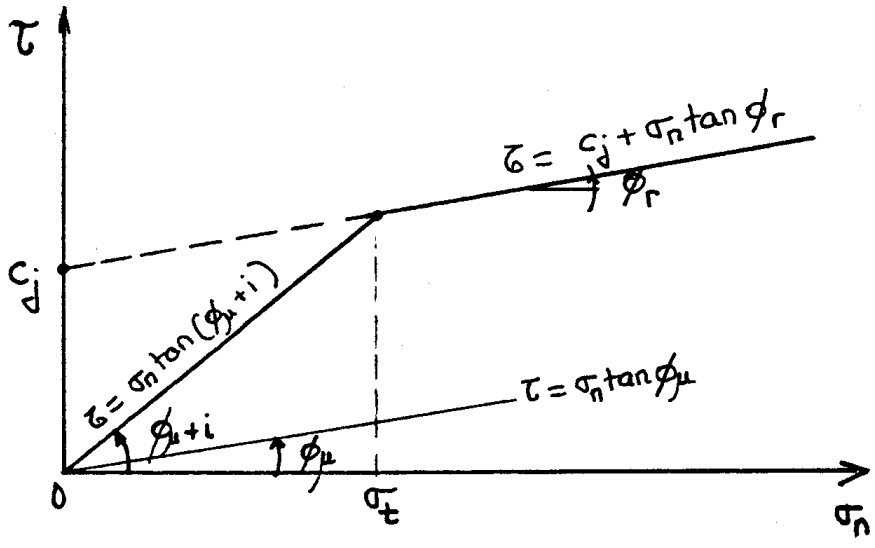

Figure 12. Patton's shear strength criterion.

where a_s and $\bar{v}$ are the proportion of total joint area sheared through the asperities and the rate of dilatancy at the peak shear strength, respectively. Both quantities are normal stress dependent and are such that

$$a_s = 1 - (1 - \frac{\sigma_n}{\sigma_T})^{k1}$$
$$\bar{v} = (1 - \frac{\sigma_n}{\sigma_T})^{k2} . \tan i_o \qquad (9)$$

where k_1 and k_2 are empirical constants with suggested values of 1.5 and 4, respectively and F_T is a transitional stress. The uniaxial compressive strength of the intact rock can be taken as an estimate to F_T. In equation (8), s_r is the shear strength of the rock comprising the asperities. It can be described by any of the intact rock strength criteria discussed in Lecture Notes 8.

3.5 Modified Ladanyi and Archambault Criterion (Saeb, 1990)

$$\tau_p = \sigma_n \tan(\phi_\mu + i)(1 - a_s) + a_s \, s_r \qquad (10)$$

This criterion emphasizes the simultaneous contribution of shearing and sliding to the shear strength of a rock joint. In equation (10), a_s is the proportion of joint surface area sheared through the asperities and (1-a_s) is the proportion on which sliding occurs. In view of equation (9), the relative contribution of shearing and sliding depends on the level of normal stress. At low normal stresses, sliding is dominant; at high normal stresses asperity shearing is dominant.

3.6 Barton and Choubey (1974)

$$\tau_p = \sigma_n \tan(\phi_b + JRC \log_{10} \frac{JCS}{\sigma_n}) \qquad (11)$$

where *JRC* is the joint roughness coefficient (see Figure 2), *JCS* is the joint wall compressive strength, and ϕ_b is the basic friction angle (also equal to ϕ_r). Examples of applications of this criterion are shown in Figure 13. Note that this criterion is very popular in practical rock engineering.

3.7 Residual Shear Strength

Goodman (1976) proposed the following model for the variation of the residual shear strength with the normal stress

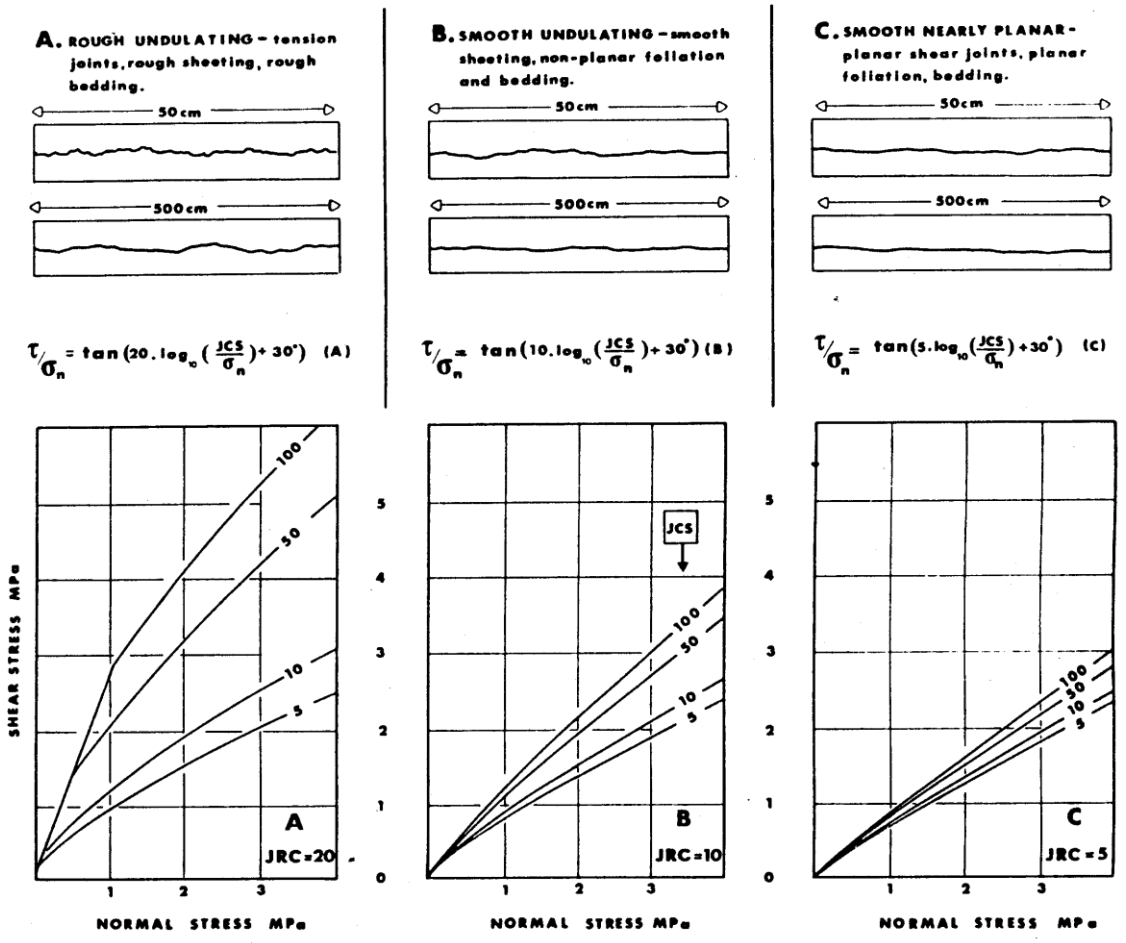

Figure 13. Examples of application of the Barton and Choubey criterion.

$$\tau_r = \tau_p\left(B_o + (1 - B_o)\frac{\sigma_n}{\sigma_T}\right) \qquad when\ \sigma_n < \sigma_T$$

$$\tau_r = \tau_p \qquad when\ \sigma_n > \sigma_T \tag{12}$$

where B_o is the ratio of peak to residual shear strength at zero (or very low) normal stress.

4. SHEAR STRENGTH OF A FRACTURED ROCK MASS

Consider an element of a regularly jointed rock mass as shown in Figure 14a. The element consists of intact rock and a joint plane and is subject to an axisymmetric and compressive state of stress (F_1, F_3). The joint plane is inclined at an angle * with respect to the direction of F_1. The shear strength of the joint is defined by the following Coulomb criterion with zero cohesion, e.g.

$$|\tau_p| = \sigma_n \tan\phi_j \tag{13}$$

Substituting the expression for F_n and J given by equation (4) into equation (13) gives the following expression for the joint shear strength in terms of F_1 and F_3

$$\sigma_1 = \sigma_3 \cdot \frac{\tan(\delta + \phi_j)}{\tan\delta} \tag{14}$$

The intact rock shear strength is assumed to be described by a Mohr Coulomb criterion with friction angle N and cohesion S_o. It can be expressed in terms of principal stresses as follows (see Lecture Notes 8)

$$\sigma_1 = C_o + \sigma_3 \frac{C_o}{T_o'} \tag{15}$$

with

$$C_o = 2S_o \tan\left(\frac{\pi}{4} + \frac{\phi}{2}\right) ; \quad \frac{C_o}{T_o'} = \tan^2\left(\frac{\pi}{4} + \frac{\phi}{2}\right) \tag{16}$$

Equations (14) and (15) have been plotted on the same diagram (F_1/C_o vs. *) in Figure 14b for N = 40°, S_o = 5 MPa, N_j = 30° and for different values of the ratio F_3/C_o. It can be seen that for values of the orientation angle * ranging essentially between 15 and 45°, slip along the joints takes place

© B. Amadei

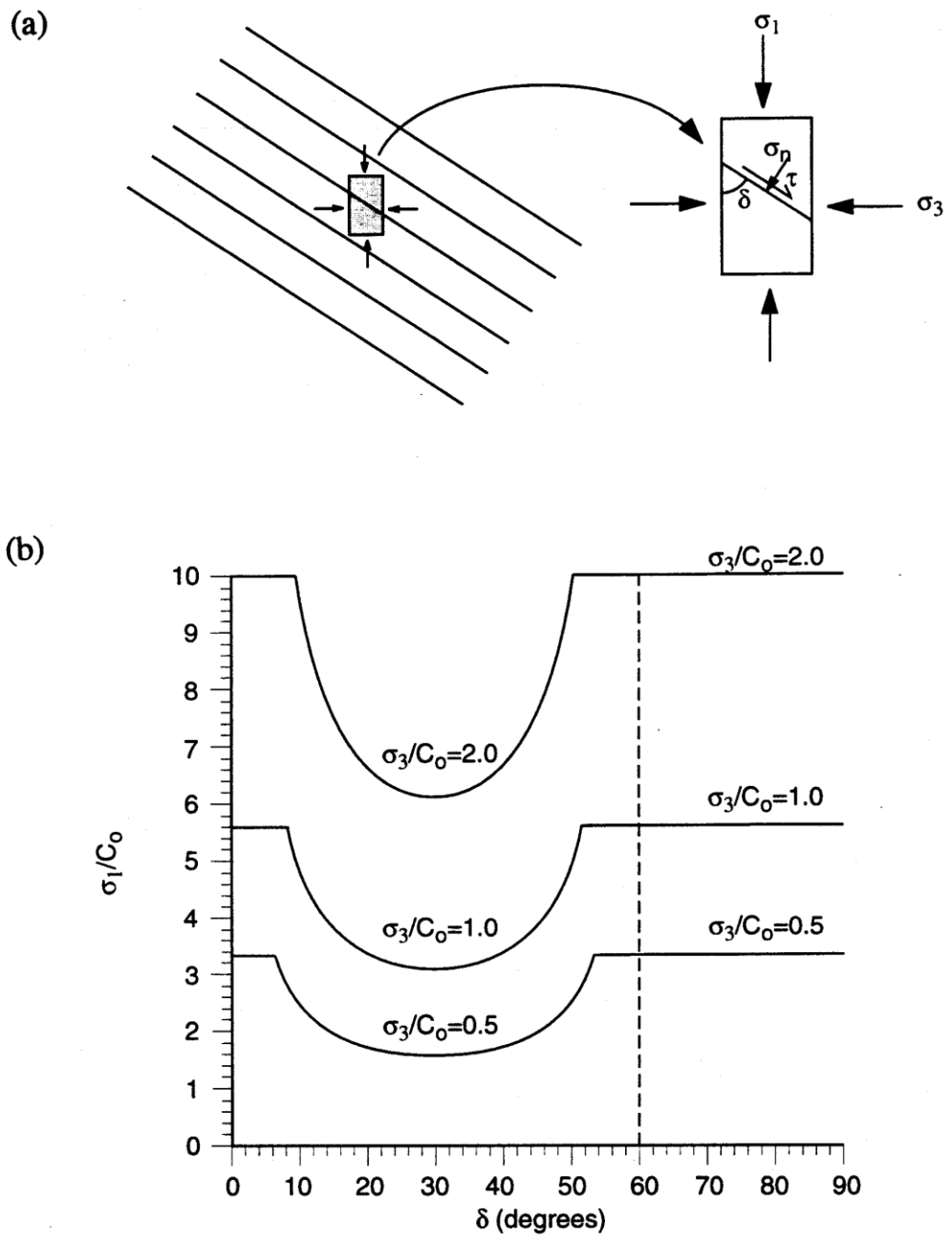

Figure 14. (a) Regularly jointed rock mass subject to an axisymmetric state of stress F_1, F_3. (b) Variation of F_1/C_o with * showing joint strength for different values of F_3/C_o. The intact rock strength is shown as a series of horizontal lines.

before the intact rock strength is mobilized. On the other hand, for small and large values of *, the shear strength of the rock mass is controlled by the intact rock. The rock mass shear strength reaches a minimum when * = 45°- $N_j/2$ = 30°.

The reduction in shear strength associated with a single joint set and illustrated in Figure 14b can be generalized for the case of multiple discontinuities as shown in Figure 15. Although the superposition principle is not correct when dealing with discontinuities, Figure 15 indicates that as the rock is cut by more and more joint sets, it behaves more like an isotropic "soil" with a uniform strength which is much less than the intact rock strength.

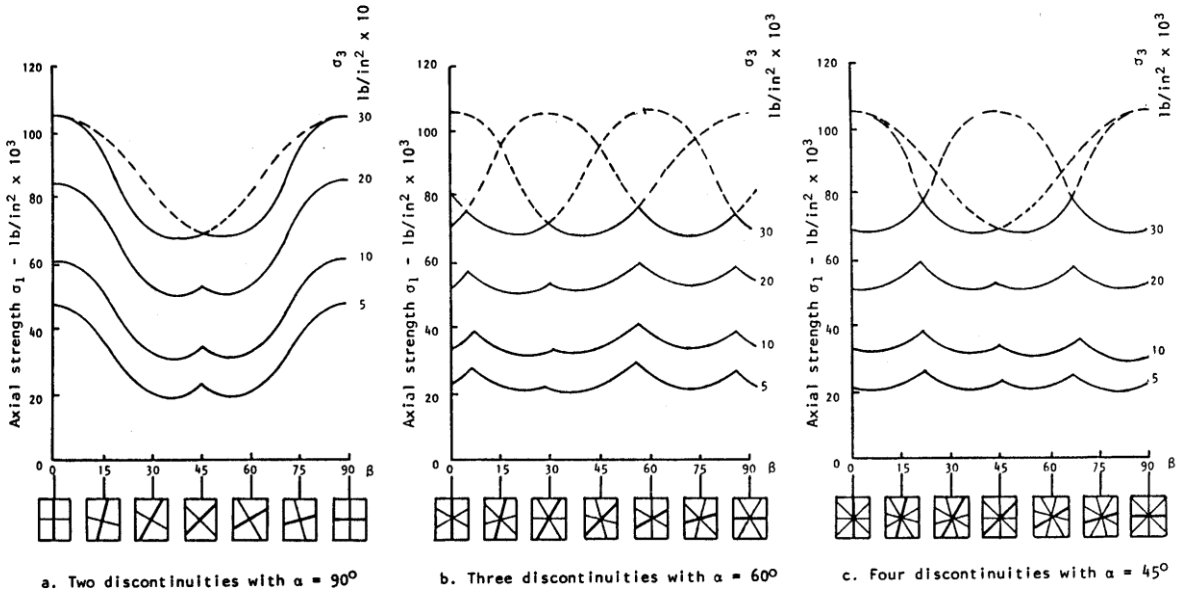

Figure 15. Strength curves for rock specimens with multiple discontinuities (after Hoek and Brown, 1980a).

5. EFFECT OF WATER ON JOINT SHEAR STRENGTH

Consider a dry joint with the orientation and the loading shown in Figure 14a. The joint has a shear strength defined by a Coulomb criterion with cohesion c_j and friction angle N_j. The joint is assumed to be stable under the applied state of stress. We propose to find the water pressure, p_w, necessary to create slip along the joint. This can be done graphically using Mohr circles as shown in Figure 16 or analytically by replacing F_1 and F_3 in equation (14) by $F_1 - p_w + H$ and $F_3 - p_w + H$, respectively with $H = c_j/\tan N_j$. The resulting equation is then solved for p_w.

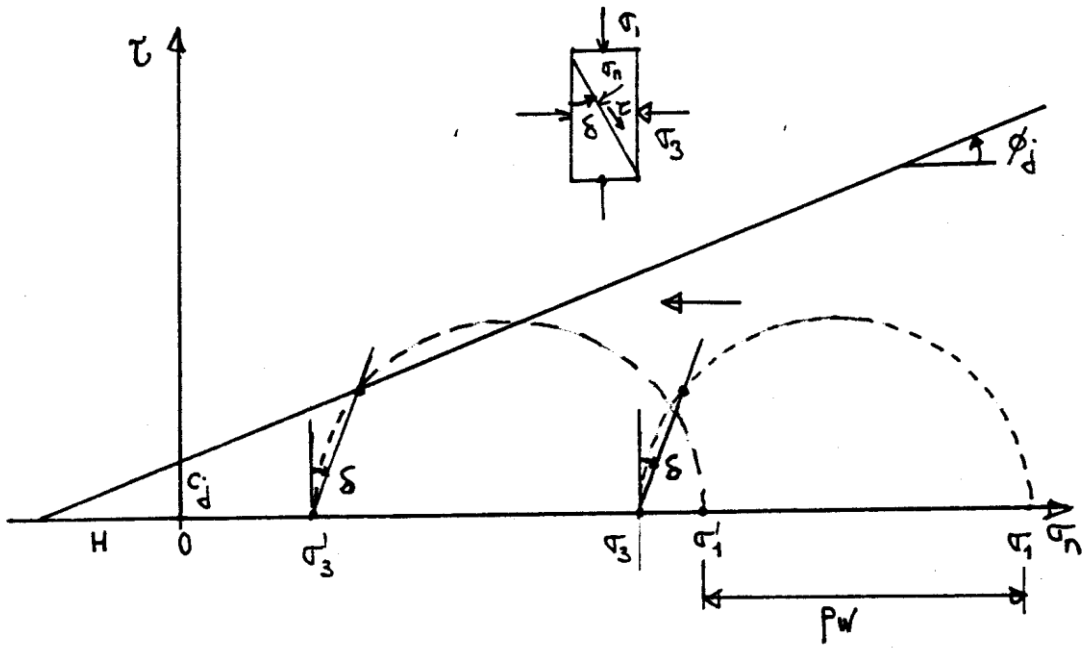

Figure 16. Slip along a joint due to an increase in water pressure.

6. HYDRAULIC PROPERTIES OF FRACTURES AND FRACTURED ROCK

Compared to intact rock, fractured rock masses are more pervious since fractures create preferred channels of water flow.

6.1 Flow in a Single Fracture

For hydraulic purpose, a fracture is often modeled as two parallel plates with a uniform aperture *b*. In the field, this aperture is indeed an average aperture obtained by drawing two mean surfaces passing through hills and over valleys of the fracture surfaces. Using fluid mechanics, it can be shown that water flow between two parallel plates can be expressed using an equation very much similar to Darcy' law for intact rock, that is

$$v = K.i \tag{17}$$

where *v* is the average velocity, *i* is the gradient of flow and *K* is a "permeability" coefficient (or hydraulic conductivity) that can be expressed as follows

$$K = \frac{gb^2}{12\nu} \tag{18}$$

where *b* is the average aperture, *g* is the acceleration due to gravity (9.81 m/s^2 or 32.2 ft/s^2) and < is the kinematic viscosity of water (1.3 x 10^{-6} m^2/s or 14 x 10^{-6} ft^2/s at 20 C°). Note that *K* has the dimensions of velocity.

Substituting the numerical values of *g* and < into equation (18) gives $K = 0.192 \times 10^6 \times b^2$ in ft/s with *b* expressed in ft. For instance, a smooth fracture with an aperture of *b* = 0.04 in (1.02 mm) will have a conductivity of 2.13 ft/s (65 cm/s) which is several order of magnitude that for intact rock.

Fracture conductivity can be measured in the laboratory using the same radial permeability apparatus used in the determination of intact rock permeability (see Lecture Notes 4). Corrections factors have been proposed by Louis (1969) to account for the effect of micro and macro surface roughness on fracture flow. Equation (18) is replaced by

$$K = \xi\frac{gb^2}{12\nu.C} \tag{19}$$

In this equation, *b* is the average crack aperture and > is the degree of crack separation. The latter varies between 0 and 1 and is defined as the ratio between the open area of the crack and its total area. In equation (19), *C* is an empirical coefficient that depends on the relative roughness of the

crack walls. The relative roughness is the ratio between the absolute roughness k (average height of crack wall asperities) and the hydraulic diameter D_h equal to $2b$ for a crack of rectangular cross section. The relative roughness varies between 0 (smooth) and 0.5 (very rough).

The coefficient C in equation (19) has been determined experimentally by Louis (1969) and is such that $C = 1$ when $k/D_h < 0.033$ and $C = 1 + (k/D_h)^{1.5}$ when $k/D_h > 0.033$. Note that equations (17)-(19) are only valid when flow in the crack is non-turbulent (laminar). For turbulent flow, more complex equations have been proposed (see Louis, 1969 and Amadei et al., 1995).

6.2 Flow in a Regularly Jointed Rock Mass

The effect of fractures on flow in a rock mass can be taken into account by using three approaches as for rock mass deformability and strength.

The first approach consists of increasing the rock mass deformability from that measured on intact rock samples in the laboratory. The second approach consists of treating each discontinuity in the rock mass as a discrete feature with a permeability given by equation (18). The third approach is to replace the fractured rock mass by an equivalent rock mass (porous medium) with anisotropic permeability properties. This approach is especially attractive when modeling regional groundwater flow where the problem domain may be very large.

Consider for instance the geometry of Figure 17a where a rock mass is cut by a joint set with spacing S. The joints have same aperture b. The intact rock permeability is K_m and the joint permeability K_j is given by equation (18). The regularly jointed rock mass can be replaced by an equivalent porous medium (Figure 17b) with permeability $K_z = K_m$ in directions normal to the joint planes and permeability $K_2 = K_m + K_j b/S$ in directions parallel to the joint planes. This approach has been generalized to more than one joint sets by several authors such as Snow (1969), Serafim and del Campo (1965) and Rocha and Francis (1977).

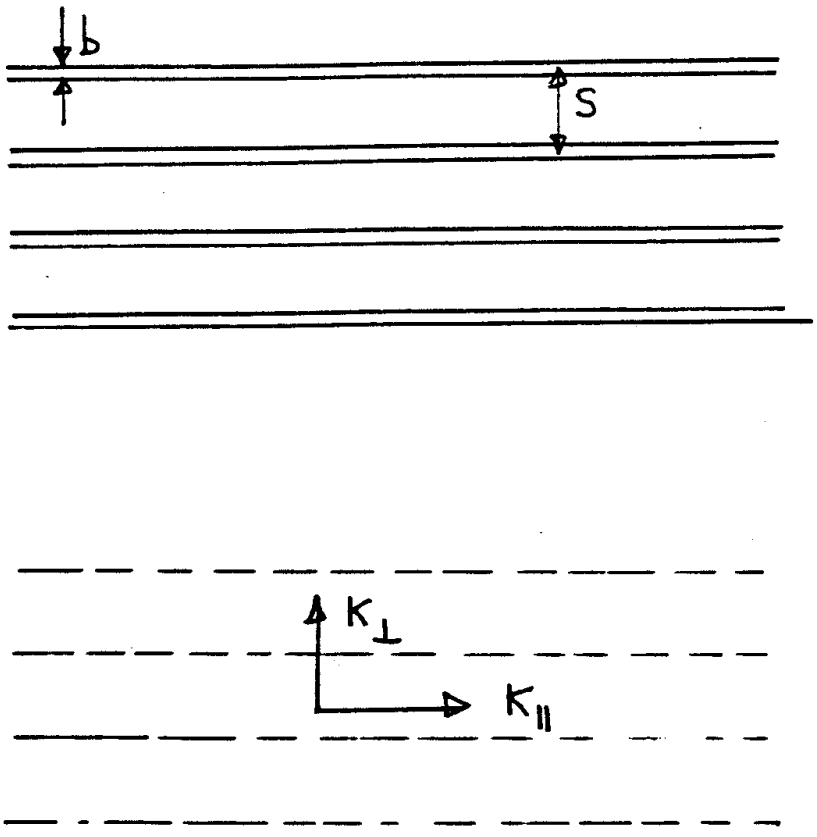

Figure 17. Flow in a regularly jointed rock mass cut by a single joint set.

7. REFERENCES

Amadei, B., Carlier, J-F. and Illangasekare, T. (1995) Effect of turbulence on fracture flow and advective transport of solutes, *Int. J. Rock Mech. Min. Sci. & Geomech. Abstr.*, Vol. 32, pp. 343-356.

Barton, N., Lien, R. and Lunde, J. (1974) Engineering classification of rock masses for the design of tunnel support. *Rock Mechanics*, **6** (4), pp. 189-236.

Barton, N. (1976) Rock mechanics review, the shear strength of rock and rock joints, *Int. J. Rock Mech. Min. Sci. & Geomech. Abstr.*, Vol. 13, pp. 255-279.

Barton, N and Choubey, V. (1977) The shear strength of rock joints in theory and practice, *Rock Mechanics*, **10**, pp. 1-54.

Bieniawski, Z.T. (1978) Determining rock mass deformability: Experience from case histories, *Int. J. Rock Mech. Min. Sci. & Geomech. Abstr.*, Vol. 15, No.5, pp. 237-248.

Bieniawski, Z.T. (1993) Classification of rock masses for engineering: the RMR system and future trends", in *Comprehensive Rock Engineering* (J.A. Hudson ed.), Pergamon, Vol. 3, pp. 553-73.

Bieniawski, Z.T. and Orr, C.M. (1976) Rapid site appraisal for dam foundations by the geomechanics classification, *Proc. 12th Int. Cong. on Large Dams*, Mexico, pp. 483-501.

Brekke, T.L. and Howard, T.R. (1973) Functional classification of gouge material from seams and faults as related to stability problems in underground openings, *Report from Univ. of Cal. to U.S. B. Mines (AD-766-046).*

Goodman, R.E. (1976) *Methods of Geological Engineering in Discontinuous Rocks*, West Publishing, St.Paul, Minnesota.

Goodman, R.E. (1989) *Introduction to Rock Mechanics*, Wiley.

Goodman, R.E. (1993) *Engineering Geology*, Wiley.

Goodman, R.E., Taylor, R.L. and Brekke, T.L. (1968) A model for the mechanics of jointed rock, *ASCE J. Soil Mech. Fnd. Div.*, **94**, SM3, pp. 637-659.

Heuze, F.E. and Barbour, T.G. (1982) New models for rock joints and interfaces. *ASCE J. Geotech. Div.*, **108**, GT5, pp. 757-776.

Heuze, F.E. (1980) Scale effects in the determination of rock mass strength and deformability, *Rock Mechanics*, Vol. 12, pp.167-192.

Hoek, E and Brown, E. T. (1980a) *Underground Excavations in Rock,* Institution of Mining and Metallurgy, London.

Hoek, E. and Brown, E.T. (1980b) Empirical strength criterion for rock masses. *ASCE J. Geotech. Eng.*, **106**, 1013-1035.

Hozik, M.J. et al. (1996) Structural Geology, in *Laboratory Manual of Physical Geology*, Prentice Hall, pp. 261-272.

Ladanyi, B. and Archambault, G. (1970) Simulation of the shear behavior of a jointed rock mass, *Proc. 11th. U.S. Symp. on Rock Mechanics*, pp. 105 - 125.

Louis, C. (1969) A Study of groundwater flow in jointed rock and its influence on the stability of rock masses, *Rock Mech. Research Report*, Imperial College, London, U.K.

Patton, F.D. (1966) Multiple modes of shear failure in rock, *Proc. 1st. ISRM Cong*., Vol 1, pp. 509-513.

Priest, S.D. and Hudson, J.A. (1976) Discontinuity spacings in rock. *Int. J. Rock Mech. Min. Sci. & Geomech. Abstr.*, Vol. 13, pp. 135-148.

Rocha, M. and Franciss, F. (1977) Determination of permeability in anisotropic rock masses from integral samples. *Rock Mechanics***, 9**, pp. 67-94.

Saeb, S. and Amadei, B. (1992) Modelling rock joints under shear and normal loading, *Int. J. Rock Mech. Min. Sci. & Geomech. Abstr.*, Vol. 29, No. 3, pp. 267-278.

Serafim, J.L. and Pereira, J.P. (1983) Considerations of the geomechanics classification of Bieniawski, *Proc. Int. Symp. on Engineering Geology and Underground Construction*, LNEC, Lisbon, Portugal, vol .1, pp. II.33-II.42.

Serafim, J.L. and del Campo, A. (1968) Interstitial pressures in rock foundations of dams, *ASCE J. Soil Mech. Foundations Div*., **91,** pp. 65-85.

Snow, D.T. (1968) Rock fracture spacings, openings and porosities, *ASCE J. Soil Mech. Foundations Div*., **94**, pp. 73-92.